Received: 7 May 2021 | Revised: 1 March 2022 | Accepted: 15 June 2022

DOI: 10.1002/mmce.23297

INTERNATIONAL JOURNAL OF RF AND MICROWAVE COMPUTER-AIDED ENGINEERING WILEY

ORIGINAL ARTICLE

A dual-band dual-sense circularly polarized self-diplexing SIW cavity-backed antenna with elliptical slot for millimeter-wave 5G applications

Amit Kumar[1] | **Munish Kumar**[2] | **Amit Kumar Singh**[1]

[1]Department of Electronics Engineering, Indian Institute of Technology (BHU), Varanasi, Uttar Pradesh, India

[2]University School of IC&T, GGS Indraprastha University, New Delhi, India

Correspondence
Amit Kumar, Department of Electronics Engineering, Indian Institute of Technology (BHU), Varanasi, India.
Email: amitk.rs.ece17@iitbhu.ac.in

Abstract

In this paper, a substrate integrated waveguide (SIW)-based circularly polarized (CP) self-diplexing antenna is proposed and discussed. The proposed antenna makes use of an elliptical slot in the metallic ground plane which is excited with the help of two separate microstrip feed lines, placed face-to-face with each other. This arrangement produces two different frequencies, centered around 21.70 and 27.10 GHz when separately excited by port-1 and port-2, respectively. The CP operation in both frequency bands can be brought by rotating the elliptical slot, which gives 3 dB axial-ratio bandwidth (ARBW) of 3.01% and 6.62% in lower and upper-frequency bands, respectively. A unidirectional radiation pattern and a peak gain of 7.70 and 9.84 dBic are obtained in lower and upper-frequency bands, respectively. The radiation efficiency of more than 80% in both the operating frequency bands has been achieved. The behavior of the cavity modes is explained using an equivalent circuit model. The proposed antenna has been fabricated and the measured results are experimentally verified with the simulated ones. The attractive features such as low profile and low weight make the proposed SIW antenna suitable for satellite and millimeter-wave 5G applications.

KEYWORDS

circular polarization (CP), diplexer, elliptical slot, substrate integrated waveguide (SIW)

1 | INTRODUCTION

Waveguides are used to transfer electromagnetic energy from one point to another with negligible losses. However, such structures are rigid and are always not desirable, and require high precision manufacturing devices.[1] Hence, the concept of substrate integrated waveguide (SIW) has, therefore, been introduced[2,3] which has emerged as one of the versatile and promising candidates in providing multiband/wideband antenna structures along with high gain.[4,5] They possess advantages for both cavity-backed (high gain/directivity levels and unidirectional radiation patterns) and planar antenna (easy fabrication and low profile).

Recently, dual-band SIW cavity backed antennas have gained attention from antenna researchers as only a single antenna can be used instead of two different ones for supporting two different frequency bands.[6] The circular polarization (CP) operation is also equally important as it eliminates the need of line-of-sight alignment of transmitter and receiver antenna systems. Also, it helps in

Abbreviations: ARBW, axial-ratio bandwidth; CP, circularly polarized; LP, linearly polarized; SIW, substrate integrated waveguide.

combating multipath-fading, and polarization mismatch issues in a wireless scenario.[7] Dual-band antennas generally have poor isolation when connected to multiple transceivers, which can be improved by using a diplexer.[8] But the introduction of this extra circuitry will increase the overall size and complexity of the antenna system. Thus, self-diplexing feature, that is, where no additional circuitry is used for multiple frequency operation was introduced due to several attractive features such as less complexity, low cost, compact size, and high isolation.[9] Several possible SIW self-diplexing antenna candidates were presented in References [10–25]. The SIW based diplexers as discussed in References [10–17] are linearly polarized (LP) with different slot shapes such as modified *U*-slot,[10,11] bowtie slot,[12] two transversely placed rectangular slots,[13] rectangular ring slot,[14] hemispherical cavity with rectangular slot,[15] half-mode SIW antenna with V-shaped slot[16] and plus-shaped slot[17] are discussed.

On the other hand, the antenna structures presented in References [18–25] are CP. In Reference [18], a dual-band CP antenna having two annular exponential slots having 3 dB axial-ratio bandwidth (ARBW) of 1.1% and 1.5% is presented. Another SIW based CP antenna, having a cavity similar to Reference [18] (rather half-size) with a spoon-shaped slot is discussed in Reference [19] shows the ARBW of up to 2.8%. Both antenna structures, as discussed in References [18,19] applies grounded coplanar waveguide (GCPW) operating in dominating TM_{010} mode. Another GCPW-fed antenna structure having an octagonal slot and a similar parasitic patch is proposed in Reference [20] shows an ARBW of 0.9% due to with chamfered corners at both slot and parasitic patch. Another SIW based coaxial-fed antenna discussed in Reference [21] where six elliptical slots of different dimensions are used to introduce the CP behavior. However, the ARBW of only 1.6% is reported. A novel idea of using an elliptical SIW cavity is explored in Reference [22] where the slot antenna shows ARBW up to 0.44% with four different arc-shaped slots. To improve the ARBW and gain,[23] implement complex additional circuitry such as quadruple ridge waveguide polarizers for obtaining CP operation and successfully achieved ARBW of 2.4%. Another coaxial probe-fed antenna with a high gain of 26.8 dBic is received in Reference [24] whereas an ARBW of the only maximum up to 1.1% is reported when 8 × 16 array is implemented. In Reference [25], SIW based CP diplexer with modified cross-slot is discussed. Here, an ARBW of 0.81% is obtained, and the structure was the first CP self-diplexing antenna with SIW technology.

In this paper, a cavity backed SIW antenna capable of supporting dual-band dual-sense CP operation is proposed for satellite broadcasting and 5G applications. The proposed antenna consists of a simple feeding network and an elliptical slot of appropriate ground plane dimensions. Further, this elliptical slot is rotated around its center, which will eventually produce CP operation in both frequency bands while maintaining the high isolation between the input ports. The generation of the perturbed cavity modes is also explained with the help of equivalent circuit analysis.

2 | ANTENNA DESIGN

2.1 | SIW cavity design

The geometrical configuration of the proposed dual-polarized SIW cavity-backed slot antenna is shown in Figure 1 where a low loss Rogers RT/Duroid 5880 copper laminated dielectric substrate material of permittivity $\varepsilon_r = 2.2$, loss tangent $\tan\delta = 0.0008$ and thickness $h = 0.787$ mm is used. The proposed antenna consists of a SIW cavity of dimension $L_{SIW} \times W_{SIW}$ as a resonator which is implemented using four rows of metallic vias of diameter d_{via}, separated by the distance p_{via} (or pitch) as depicted in Figure 1A.

The value of d_{via} and p_{via} is chosen in such a way that there will be minimum radiation loss and leakage of energy and given by.[26]

$$\frac{p_{via}}{d_{via}} < 2 \tag{1a}$$

$$d_{via} < \frac{\lambda_g}{5} \tag{1b}$$

The relationship between the resonance frequency for any TE_{mnp} of the SIW cavity formed by the metallic vias and geometrical parameters related to the proposed antenna dimensions can be calculated as follows.[27]

$$f_r = \frac{c}{2\sqrt{\varepsilon_r}}\sqrt{\left(\frac{m}{W_{eff}}\right)^2 + \left(\frac{n}{L_{eff}}\right)^2 + \left(\frac{p}{h}\right)^2} \tag{2a}$$

$$W_{eff}/L_{eff} = W_{SIW}/L_{SIW} - \frac{1.08p_{via}^2}{d_{via}} + \frac{0.1p_{via}^2}{W_{SIW}/L_{SIW}} \tag{2b}$$

where the terms m, n, p are the modal indices. The dimensions of the SIW cavity are chosen in such a way that they support and keep the dominant TE_{110} mode within the upper 5G band. Two separate microstrip lines having characteristic impedance of 50 Ω are used for excitation and make the connections of 50 Ω SMA connectors straightforward.

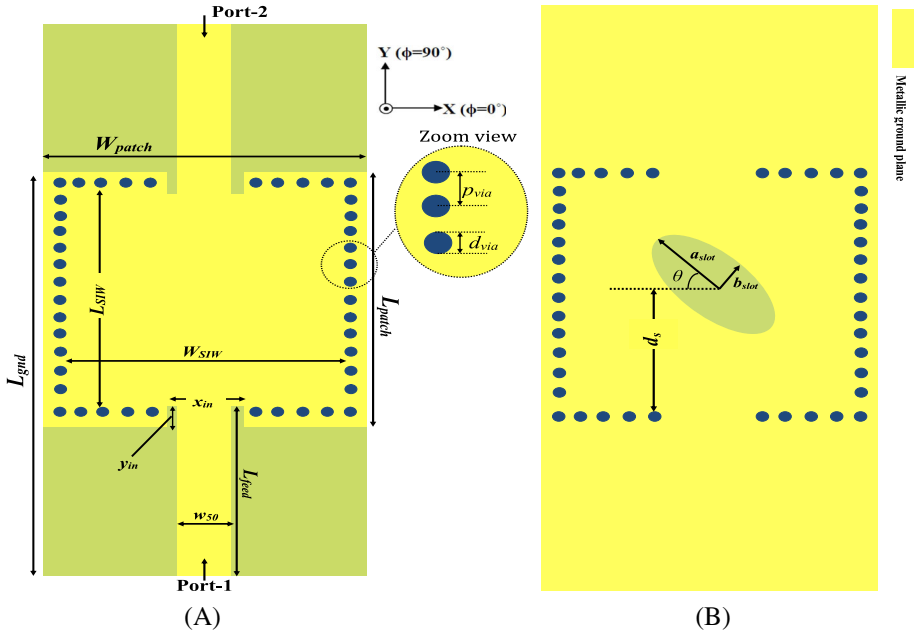

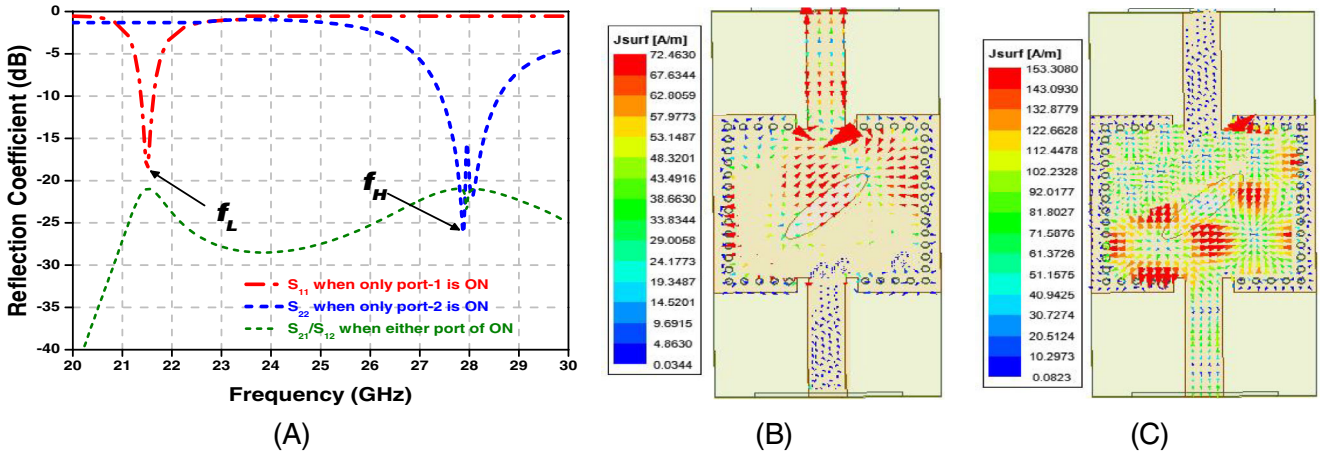

FIGURE 1 Schematic of the proposed antenna. (A) Top view (B) Bottom view. $W_{patch} = 12$, $L_{patch} = 12$, $L_{gnd} = 19$, $W_{SIW} = 10.40$, $L_{SIW} = 10.40$, $w_{50} = 2$, $L_{feed} = 8$, $y_{in} = 1$, $x_{in} = 3.20$, $p_{via} = 0.80$, $d_s = 5$, and $d_{via} = 0.40$. All dimensions are in "mm"

FIGURE 2 (A) S_{11} of the proposed antenna when excited separately with each port; surface current density at (B) 21.50 GHz and (C) 28.05 GHz, when excited only with port-1 and port-2, respectively. f_L (=21.50 GHz) and f_H (=28.05 GHz) are the operating frequency bands generated when excited either with port-1 or port-2, respectively.

An elliptical slot is etched in the metallic ground plane at an offset distance of d_s ($\neq \frac{L_{SIW}}{2}$) from the center as shown in Figure 1B. The asymmetric position of the elliptical slot divides the whole SIW cavity into two unequal parts. This will generate two different resonant modes due to perturbed electric field ($\vec{E}$) when excited separately with port-1 and 2 as shown in Figure 2A. The frequency bands generated are centered around 21.50 GHz (21.37–21.64 GHz; 1.26%) and 28.05 GHz (27.42–28.63 GHz; 4.32%). The surface current distribution at 21.50 and 28.05 GHz frequency bands is shown in Figure 2B,C, respectively.

Figure 2B shows the surface current which is mainly concentrated in the upper-half of the SIW cavity while excited with port-1 only. Similarly, when port-2 is excited, the current density mainly concentrates only around lower-half of the SIW cavity. The electric field generated around the elliptical slot when excited either with port-1 or port-2 are out-of-phase with each other and hence, helps the proposed SIW cavity antenna to radiate into the free space as a dual-port dual-band antenna. The longitudinal placement of elliptical slot prevents the spilling of electromagnetic waves from one port to other. The negligible transmission (S_{12}/S_{21}) from one

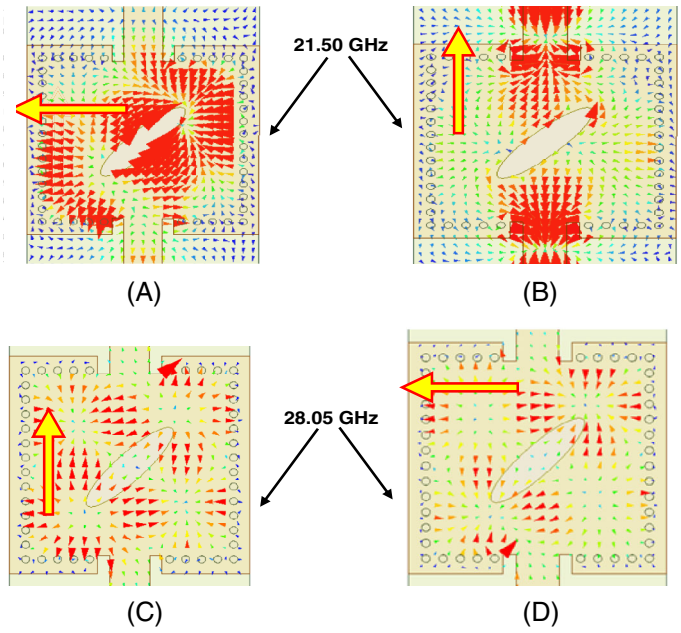

FIGURE 3 Plots of vector surface current density (A) $\omega t = 0°$, (B) $\omega t = 90°$ taken at 21.50 GHz and (C) $\omega t = 0°$, (b) $\omega t = 90°$ taken at 28.05 GHz when excited from port-1 and port-2, respectively.

port to other as depicted from Figure 2A (green dotted line) enhances the isolation between them.

2.2 | Effect of elliptical slot

A rotated elliptical slot having semi-major axis a_{slot} and rotation angle θ is etched in the ground plane as shown in Figure 1B due to which the SIW cavity is segmented into two unequal resonators. The dual-frequency ($f_{11}^{even,odd}$) corresponding to dominant $TM_{11}^{even,odd}$ mode of an elliptical slot of given eccentricity and semi-major axis is given by.[28]

$$\left(f_{11}^{even,odd}\right) = \frac{15}{\pi e_{slot} a_{slot}} \sqrt{\frac{q_{11}^{even,odd}}{\varepsilon_r}} \tag{3}$$

where $e_{slot}\left(= \sqrt{1 - \left(\frac{b_{slot}}{a_{slot}}\right)^2}\right)$ is the eccentricity of the elliptical slot, b_{slot} is the semi-minor axis length, $q_{11}^{e,o}$ is an approximated Mathieu function which can be calculated as follows.[29]

$$q_{11}^{even} = -0.0049 e_{slot} + 3.7888 e_{slot}^2 - 0.7228 e_{slot}^3 + 2.2314 e_{slot}^4 \tag{4a}$$

$$q_{11}^{odd} = -0.0063 e_{slot} + 3.8316 e_{slot}^2 - 1.1351 e_{slot}^3 + 5.2229 e_{slot}^4 \tag{4b}$$

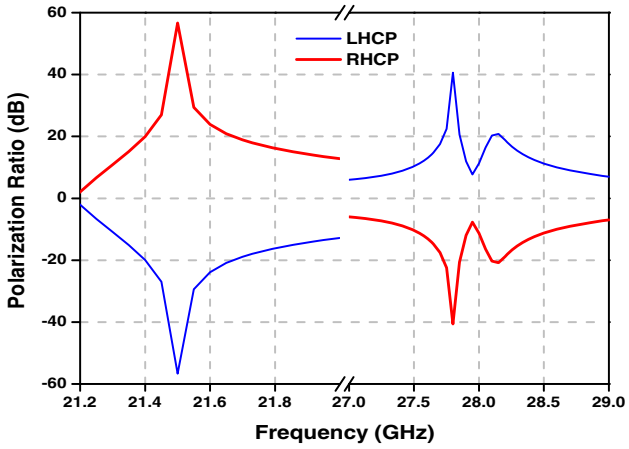

FIGURE 4 Polarization conversion ratio (PCR) for the proposed SIW antenna

The elliptical slot present in the metallic ground plane is rotated around its center (having rotation angle θ as shown in Figure 1B) that generates two orthogonal $\vec{E}$-field vectors of almost equal amplitude and phase difference of 90° and hence CP operation is obtained. The variation in distance d_s and rotation angle θ helps in achieving wide axial-ratio bandwidth (ARBW) in both lower and upper frequency bands. Figure 3 shows the vector surface current distribution ($\vec{J}$) at 21.50 and 28.05 GHz when excited from port-1 and port-2, respectively. It is evident that the proposed antenna shows RHCP behavior (clockwise movement of $\vec{J}$) when excited with port-1 and LHCP when excited with port-2 (anticlockwise movement of $\vec{J}$). Furthermore, the purity of LHCP/RHCP behavior can also be confirmed from polarization conversion ratio (PCR), which can be defined as

$$PCR = r_{xy}^2 / \left(r_{xy}^2 + r_{yy}^2\right) \tag{5}$$

where $r_{xy} = |\overrightarrow{E_x^r} / \overrightarrow{E_y^i}|$ and $r_{yy} = |\overrightarrow{E_y^r} / \overrightarrow{E_y^i}|$ represent the ratio of E-field in y-to-x and y-to-y polarization conversion, respectively.[30] The magnitude of RHCP is remarkably higher than LHCP magnitude in lower frequency band and that of LHCP than RHCP in upper frequency band as shown in Figure 4.

3 | EQUIVALENT CIRCUIT MODEL

To understand the propagating modes within the SIW cavity, the proposed antenna is analyzed with the help of equivalent circuit model. A keysight advanced design system (ADS) software is used to simulate and optimize the

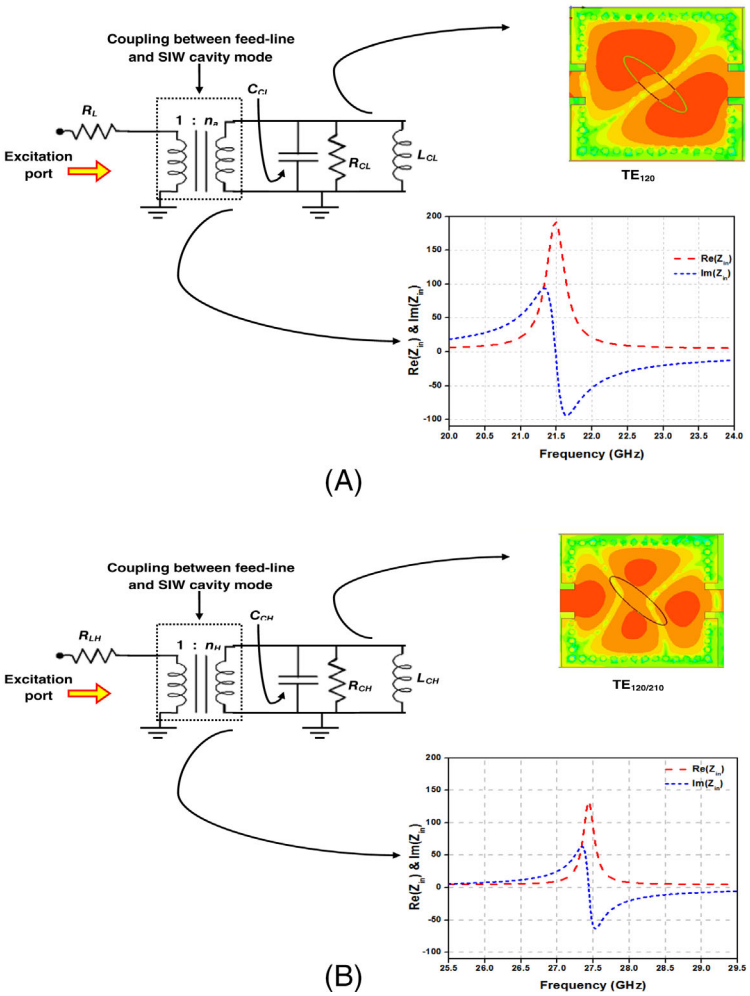

FIGURE 5 Equivalent circuit model of the proposed antenna for (A) lower and (B) higher resonant mode. The modal parameters are $n_a = 18.29$, $C_{CL} = 8.08$ fF, $R_{CL} = 63$ KΩ, $L_{CL} = 6.79$ nH, $n_H = 25$, $C_{CL} = 11$ fF, $R_{CL} = 80.26$ KΩ, $L_{CL} = 3.05$ nH, and $R_L = 4.68$ Ω

equivalent circuit of the proposed SIW cavity antenna. The SIW cavity can be modeled as a parallel combination of LCR resonant circuit corresponding to each propagating resonating mode.[31] Therefore, the frequency bands generated around 21 and 28 GHz can be modeled as three parallel LCR circuits where n_a, L_{CL}, C_{CL} and R_{CL} corresponds to lower 21.50 GHz resonant mode while n_H, L_{CH}, C_{CH}, and R_{CH} corresponds to higher 28.05 GHz frequency bands as shown in Figure 5.

4 | PARAMETRIC STUDY

As discussed in previous sections, the resonating frequencies obtained depend mainly on cavity and slot dimensions. Also, slot position can also be changed to tune the lower and upper frequencies (or f_H/f_L) and to obtain high level of isolation between the input ports. Here, the effect of distance d_S, rotation angle θ and slot dimensions in terms of eccentricity e on antenna matching characteristics is discussed.

4.1 | Effect of distance d_s

Both lower and upper resonant frequencies of the proposed antenna vary with the change in the position of the slot position d_s as shown in Figure 6A. It is observed that the lower resonant frequency decreases from 22.06 to 21.50 GHz while upper resonant frequency increases from 27.87 to 28.50 GHz with increase in distance d_s from 3 to 6 mm. Correspondingly, the frequency ratio $(=\frac{f_H}{f_L})$ varies from 1.26 to 1.33 while maintaining a good level of isolation (or $S_{21} \geq 22$ dB) between the input ports.

4.2 | Effect of rotation angle, θ of elliptical slot

The elliptical slot is rotated around its center in order to bring the CP operation in the desired frequency bands. The effect of rotation angle θ on matching characteristics is shown in Figure 6B. It is evident that as θ goes from 0° to 60°, the lower and upper resonating frequencies shifts from

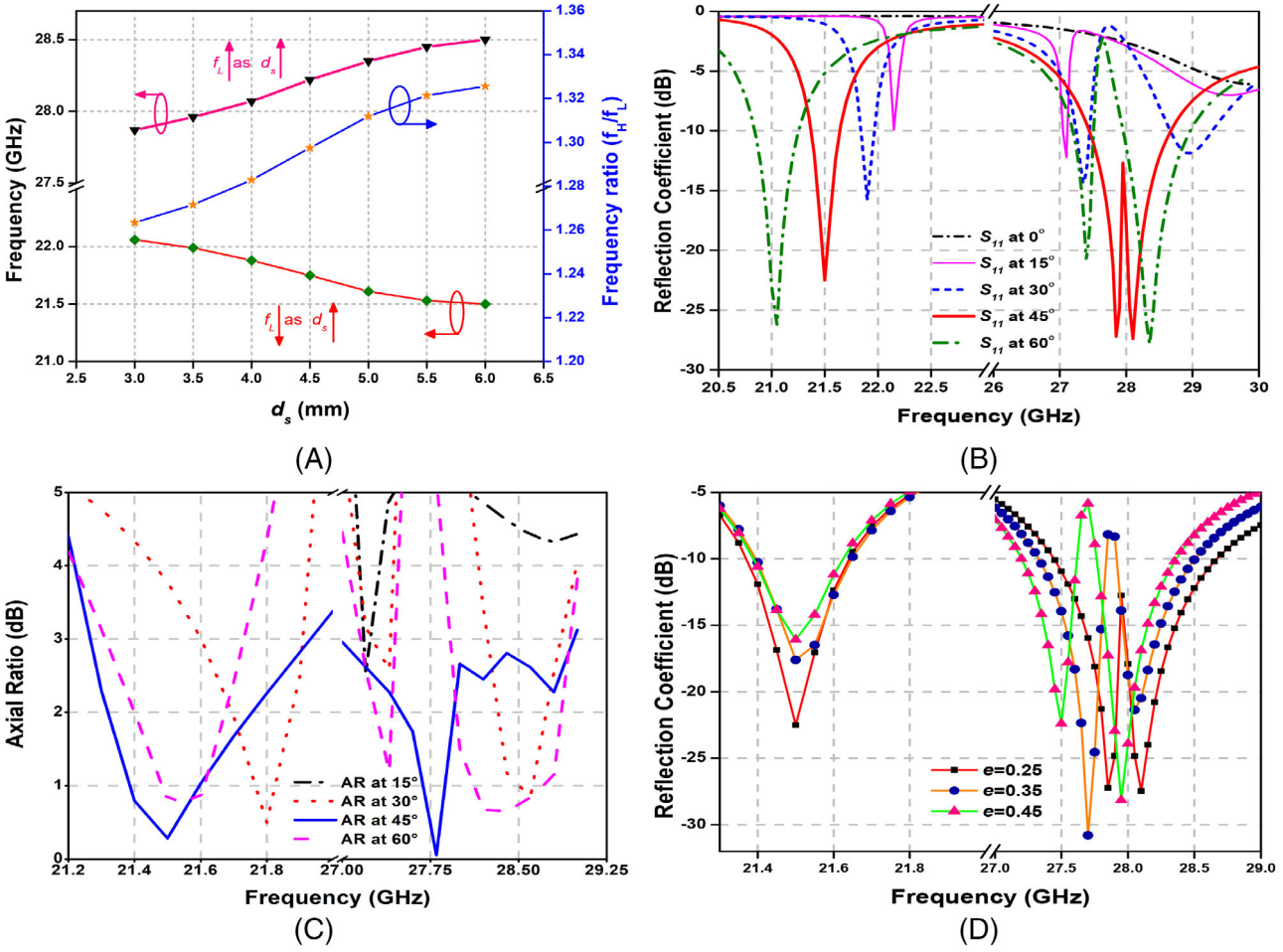

FIGURE 6 Effect of (A) distance d_s, (B) rotation angle θ with S_{11}, (C) rotation angle θ with AR and (D) eccentricity of elliptical slot on matching characteristics

20.95 to 21.05 GHz and 27.10 to 28.35 GHz, respectively. The percentage bandwidth in lower and upper frequency bands shifts from 0% to 1.39% and 0.37% to 4.28% as θ varies from 0° to 45°. At $\theta = 60°$, the upper band splits into two separate frequency bands, centered around 27.40 and 28.35 GHz whereas lower frequency bands shifts to 21.05 GHz. The another effect of rotation angle θ on axial ratio is illustrated in Figure 6C. At $\theta = 0°$, no CP operation is seen in both upper and lower frequency bands. As θ approaches to 15°, CP in only upper resonating frequency (around 27.2 GHz) is seen as depicted from Figure 6C. For further increase in θ, the maximum ARBW of 3.01% and 6.62% for lower and upper frequency bands, respectively, is reported at $\theta = 45°$. As θ reaches to 60°, the ARBW goes down to 2.73% and no CP operation is seen beyond 60°.

4.3 | Effect of eccentricity, *e* of elliptical slot

The effect of eccentricity e of the elliptical slot on matching characteristics is shown in Figure 6D. It is observed that the effect of e is negligible on lower frequency band whereas the upper frequency band divides into two as e goes from 0.25 to 0.45 (or becomes more like a circle).

5 | EXPERIMENTAL RESULTS AND DISCUSSION

5.1 | Matching characteristics

The photograph of the fabricated prototype (front side, back side and having the SMA connectors while testing) of the proposed SIW cavity antenna is shown in Figure 7A. The Keysight N9951A FieldFox Microwave Analyzer is used to measure all S-parameters of the proposed antenna. The comparison of the simulated and measured S-parameters of the proposed antenna is illustrated in Figure 7B. The measured results show that the proposed antenna supports two different frequency bands, that is, within 21.38–21.92 GHz (2.49%) and 26.68–27.58 GHz (3.32%) frequency bands, S_{11} is below −10 dB.

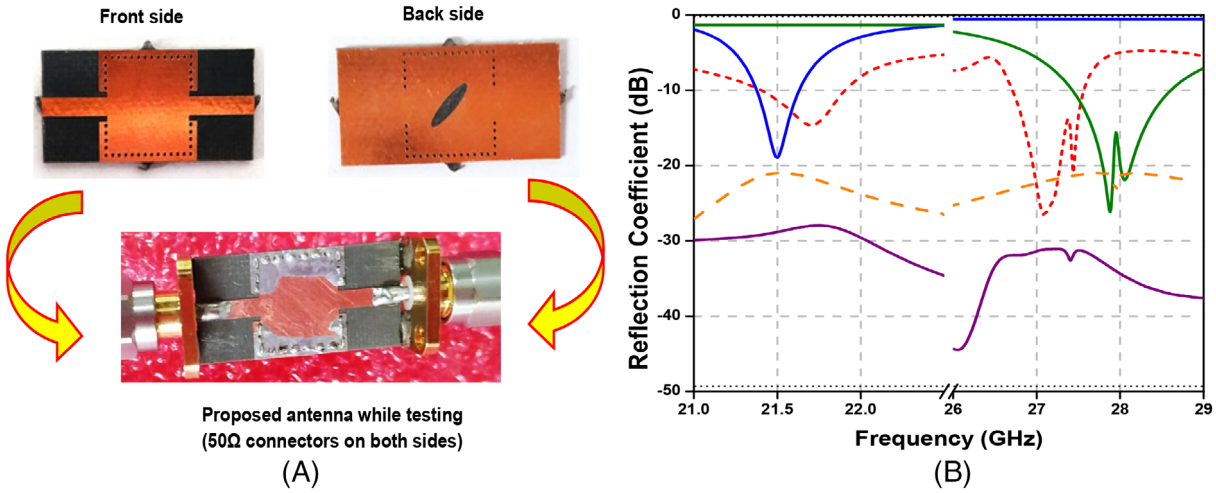

FIGURE 7 (A) Fabricated version of the proposed SIW antenna and (B) simulated S_{11}, S_{22} and S_{12}/S_{21} of the proposed SIW antenna. (i) Solid blue line: simulated S_{11} when only port-1 is ON; (ii) solid green line: simulated S_{11} when only port-2 is ON; (iii) solid violet line: simulated S_{12}/S_{21}; (iv) orange dotted line: measured S_{12}/S_{21}; (v) red dotted line: measured S_{11} when either port is ON.

FIGURE 8 (A) Proposed SIW cavity-backed antenna inside anechoic chamber during gain/efficiency and radiation pattern measurement; simulated/measured and (B) gain/radiation efficiency

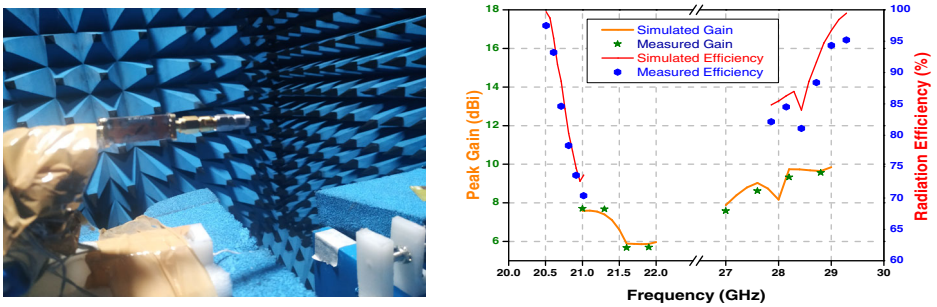

5.2 | Gain, efficiency, and radiation pattern characteristics

The measurements related to gain, efficiency and radiation pattern are performed inside the properly calibrated anechoic chamber where a horn antenna of known gain is placed at a distance of 8.1 m away from the proposed antenna (whose gain/radiation pattern has to be measured). The measurement setup for the same is shown in Figure 8A.

The peak gain and efficiency are measured for the given operating frequency band against frequency at $\theta = \phi = 0^{\circ}$ as shown in Figure 8B. The peak gain varies from 5.69 to 7.70 dBic with an average gain of 6.69 dBic within the lower operating frequency band. Also, the peak gain varies from 7.88 to 9.84 dBic with an average gain of 8.77 dBic within the upper operating frequency range. Figure 8B also shows the radiation efficiency of the proposed wide-slot antenna. It is seen that the radiation efficiency at $\theta = \phi = 0^{\circ}$ varies from 70.37% to 97.49% and 82.16% to 95.19% within the lower and upper operating frequency range, respectively. The average radiation efficiency within lower and upper operating frequency range is 82.95% and 87.62%, respectively.

The radiation patterns of the proposed antenna in *YZ*-plane ($\phi = 0^{\circ}$) and *XZ*-plane ($\phi = 90^{\circ}$) at 21.70 and 27.10 GHz (resonating frequencies of lower and upper frequency bands) are plotted in Figure 9. It is evident from Figure 9 that measured results are in good agreement with corresponding simulated patterns. A small inconsistency in both the results due to fabrication imperfection may be attributed. It is also observed that an isolation of >22 dB in both frequency bands is obtained. The measured cross-polarization is about (38, 40 dB) in *YZ*-plane and (31, 38 dB) in *XZ*-plane at the frequencies 21.70 and 27.10 GHz, respectively. The front-to-back ratio (FTBR) in all cases is better than 15 dB.

5.3 | Axial-ratio versus frequency

The measured 3-dB ARBW for both the frequency bands of the proposed SIW cavity antenna is about

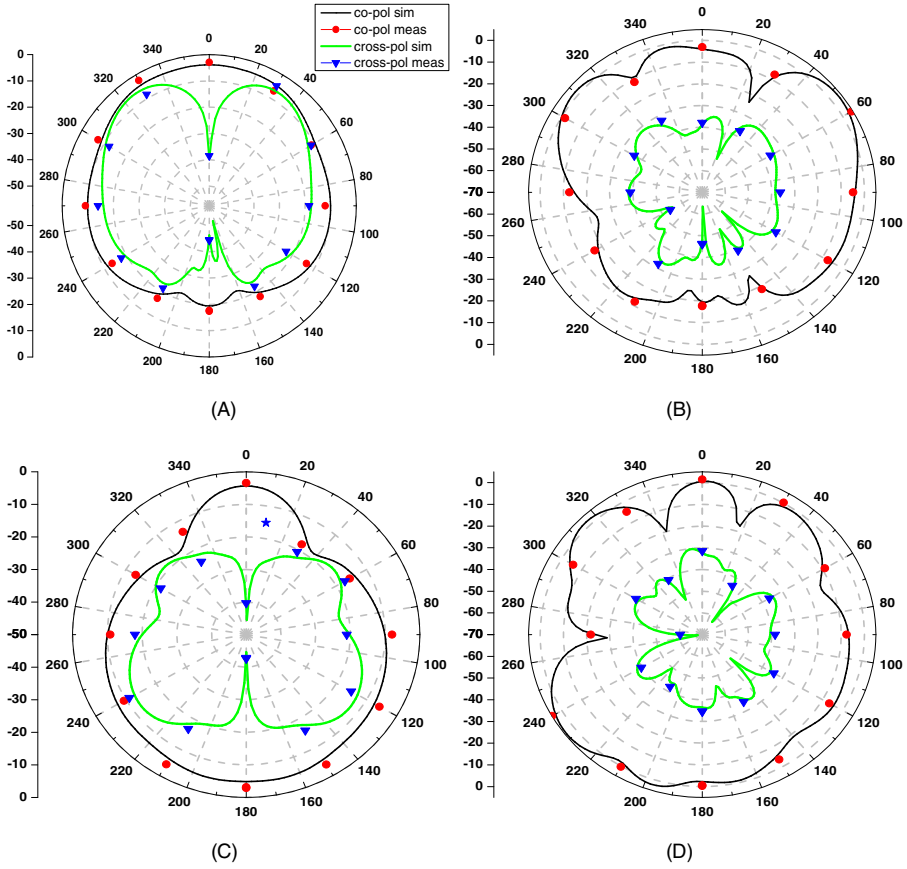

FIGURE 9 Simulated and measured radiation patterns (A) $\phi = 0^{\circ}$, (B) $\phi = 90^{\circ}$ at 21.70 GHz when excited with port-1 only; (C) $\phi = 0^{\circ}$, (D) $\phi = 90^{\circ}$ at 27.10 GHz when excited with port-2 only

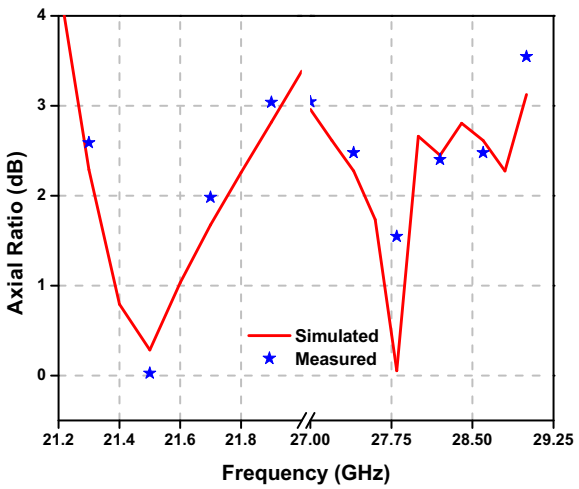

FIGURE 10 Simulated versus measured axial-ratio of the proposed antenna

650 MHz (21.25–21.90 GHz) and 1850 MHz (27–28.85 GHz) at $\theta = \phi = 0^{\circ}$ is shown in Figure 10. The measured percentage ARBW for both frequency bands is 3.01% and 6.62% which lies slightly out of the measured operating frequency range. The minimum axial ratio of 0.02 and 0.52 dB at 21.5 and 27.80 GHz, respectively, is obtained.

6 | COMPARISON ANALYSIS

Table 1 shows the comparison of the proposed dual-band dual-sense CP SIW antenna with other reported SIW based diplexers and CP antenna structures. The main contributions of the proposed work along with its comparison with existing antenna structures as discussed in this paper are as follows:

6.1 | Linearly polarized SIW diplexers

1. *Comparison in terms of size*: The proposed antenna possesses more compact physical dimensions as compared to antenna structures reported in References [10–17]. This is achieved due to the perturbation of dominant TE_{110} and hybrid mode generated due to merging of TE_{130} and TE_{310} modes. These degenerated modes arise due to loading of elliptical slot on the SIW cavity.
2. *Comparison in terms of impedance bandwidth*: The proposed antenna has highest 10 dB impedance bandwidth (IBW) among SIW based diplexers reported in References [10–17] except [11]. However, the peak gain and maximum radiation efficiency of the proposed antenna is about 4.29 dB and 33.49%,

TABLE 1 Comparison with other SIW based diplexers present in the literature

LP/CP antenna	Parameters		10		12		11		13		14		15		16		17	
	Excitation port		Port-1	Port-2	Port-1	Port-2	Port-1	Port-2	Port-1	Port-2	Port-1	Port-2	Port-1	Port-2	Port-1	Port-2	Port-1	Port-2
LP	10 dB IBW	GHz	4.26–4.31	7.47–7.60	NR		3.9–4.37	4.63–5.34	8.22–8.36	10.32–10.6	NR		5.11–5.23	5.75–5.89	NR		8.47–8.63	9.71–9.83
		%	1.16	1.72	NR		11.30	14.24	1.93	2.68	1.32	1.46	2.32	2.40	NR		1.04	0.91
	Isolation (dB)		>40.5	>32.2	25		NR		29.2	30.2	29		33.2	33.8	22.2	25.7	20	18
	Gain (dBi)		5.38	5.82	4.3	4.2	3.82	4.48	3.56	5.24	5.75	5.95	3.31	4.16	4.0	4.3	5.7	5.9
	Size (mm^2)		NR		NR		38 × 38		32 × 26		NR		NR		NR		NR	
	Radiation Efficiency (%)		95.1	95.1	NR		65	64	NR		NR		60	70	NR		NR	
CP	Parameters		18	19	20	21	22	23	24	25		This work						
	10 dB IBW	GHz	37.25–37.25	27.25–28.53	5.8	12.09–12.6	5.65–5.78	34.67–35.15	11.87–12.19	12.15–12.38	11.48–11.91	21.38–21.92	26.68–27.58					
		%	1.1	6.3	2.4/2.6	4.2	1.16	1.5	2.7	1.87	3.67	2.49	3.32					
	3 dB ARBW	GHz	37–37.4	27.85–28.25	NR	-	5.7–5.72	34.52–35.38	12–12.11	12.27–12.37	11.67–11.86	21.25–21.9	27–28.85					
		%	1.1	1.8	0.9	1.6	0.35	2.4	0.9	0.81	1.61	3.01	6.62					
	Isolation (dB)		NR		NR	NR	NR	NR	NR	18.52	14.05	>22	>22					
	Gain (dBic)		5	5.9	6.57/6.98	7.4	7.96	18.14	8.49	5.6	5.9	6.69	8.77					
	Size (mm^2)		NR	37 × 37	NR	NR	NR	NR	16.2 × 16.2	NR		26 × 12						
	Radiation Efficiency (%)		88	NR	86.8/87	NR	NR	NR	NR	NR		82.95	87.62					
	Polarization State:		LHCP	RHCP	RHCP	LHCP	RHCP	RHCP	RHCP/LHCP	RHCP	LHCP	RHCP	LHCP					
	Technique Used:		Two annular slots	Spoon-shaped slot	Chamfered cornered patch	Multiple elliptical slots	Arc-shaped slot	Rotated Koch slot	Rectangular slots	Asymmetric cross-slot		Elliptical slot						

Abbreviation: NR, not reported.

respectively, better than the antenna structure reported in Reference [11].
3. *Overall advantage*: The proposed antenna exhibits self-diplexing mechanism along with flexibility in tuning frequency ratio from 1.26 to 1.33, compact size, high gain, high isolation of more than 22 dB and front-to-back ratio (FTBR) of more than 15 dB in both frequency bands.

6.2 | Circularly polarized SIW antennas

1. The proposed antenna shows simple geometry, high 10 dB IBW, compact size among the SIW based antenna structures reported in References [18–25].
2. The 3 dB ARBW of the proposed antenna is also highest among the antennas discussed in References [18–25].
3. The proposed antenna shows both LHCP and RHCP polarization states whereas the antenna structures reported in References [18–23] either show LHCP or RHCP polarization state.
4. *Overall advantage*: The proposed antenna is best suited for 5G applications including 26.50–27.50 GHz in Italy and Switzerland, 26 GHz in Germany and France, 24.25–27.50 GHz in India. In 21.38–21.90 GHz in amateur satellite, broadcasting, and Amateur radio operators which includes terrestrial, satellites and planetary communications.

7 | CONCLUSION

A compact self-diplexing circularly polarized (CP) SIW antenna with an elliptical slot is presented. Initially, an elliptical slot is etched in the metallic ground plane, and its proper positioning (i.e., distance d_s) helps in achieving dual-band operation, that is, centered around 21 and 28 GHz. The rotation of the elliptical slot helps in producing two orthogonal electric field vectors of almost equal amplitude and phase difference of 90°, thereby achieves CP operation in both frequency bands. Proper tuning of elliptical slot dimensions and rotation angle are the two factors that affect the 3 dB axial-ratio bandwidth (ARBW) of the proposed antenna. Measured results show that the proposed antenna exhibits dual-band operation in 21.38–21.92 GHz (2.49%) and 26.68–27.58 GHz (3.32%) along with corresponding ARBW of 21.25–21.90 GHz (3.01%) and 27–28.85 GHz (6.62%), respectively. Due to the SIW cavity, the proposed antenna shows a unidirectional radiation pattern with a gain more than 5 dBic and isolation better than 22 dB in both the frequency bands. This makes the proposed antenna an attractive/suitable candidate for both satellite broadcasting and 5G applications.

DATA AVAILABILITY STATEMENT

Data sharing is not applicable to this article as no new data were created or analyzed in this study.

ORCID

Amit Kumar https://orcid.org/0000-0002-8533-2236
Munish Kumar https://orcid.org/0000-0003-0263-0009
Amit Kumar Singh https://orcid.org/0000-0002-4246-7608

REFERENCES

1. Llamas-Garro I, Corona-Chavez A. Micromachined transmission lines for millimeter-wave applications; 2006, p. 15.
2. Uchimura H, Takenoshita T, Fujii M. Development of a "laminated waveguide". *IEEE Trans Microw Theory Tech*. 1998; 46(12):2438-2443. doi:10.1109/22.739232
3. Cheng S, Kratz KH, Yousef HA. Substrate integrated waveguide; 2011. https://patents.google.com/patent/US20110018657A1/en
4. Wu K, Bozzi M, Fonseca NJG. Substrate integrated transmission lines: review and applications. *IEEE J Microw*. 2021;1(1): 345-363. doi:10.1109/JMW.2020.3034379
5. Kumar A, Kumar M, Singh AK. Substrate integrated waveguide cavity backed wideband slot antenna for 5G applications. *Radioengineering*. 2021;30(3):480-487. doi:10.13164/re.2021.0480
6. Omar AA, Scardelletti MC, Hejazi ZM, Dib N. Design and measurement of self-matched dual-frequency coplanar waveguide-fed-slot antennas. *IEEE Trans Antennas Propag*. 2007;55(1): 223-226. doi:10.1109/TAP.2006.888475
7. Kumar M, Nath V. A circularly polarized printed elliptical wide-slot antenna with highbandwidth-dimension-ratio for wireless applications. *Wirel Netw*. 2020;26:5485-5499. doi:10.1007/s11276-020-02399-9
8. Strassner B, Chang K. Wide-band low-loss high-isolation microstrip periodic-stub diplexer for multiple-frequency applications. *IEEE Trans Microw Theory Tech*. 2001;49(10):1818-1820. doi:10.1109/22.954789
9. Lu Y, Lin Y. A mode-based design method for dual-band and self-Diplexing antennas using double T-stubs loaded aperture. *IEEE Trans Antennas Propag*. 2012;60(12):5596-5603. doi:10.1109/TAP.2012.2211852
10. Barik RK, Cheng QS, Dash SKK, Pradhan NC, Karthikeyan SS. Compact high-isolation self-diplexing antenna based on SIW for C-band applications. *J Electromagn Waves Appl*. 2020;34(7):960-974. doi:10.1080/09205071.2020.1763859
11. Boukarkar A, Lin XQ, Jiang Y, Yu YQ. A tunable dual-fed self-diplexing patch antenna. *IEEE Trans Antennas Propag*. 2017; 65(6):2874-2879. doi:10.1109/TAP.2017.2689035
12. Mukherjee S, Biswas A. Design of self-diplexing substrate integrated waveguide cavity-backed slot antenna. *IEEE Antennas Wirel Propag Lett*. 2016;15:1775-1778. doi:10.1109/LAWP.2016.2535169

13. Nandi S, Mohan A. An SIW cavity-backed self-Diplexing antenna. *IEEE Antennas Wirel Propag Lett*. 2017;16:2708-2711. doi:10.1109/LAWP.2017.2743017
14. Khan AA, Mandal MK. Compact self-diplexing antenna using dual-mode SIW square cavity. *IEEE Antennas Wirel Propag Lett*. 2019;18(2):343-347. doi:10.1109/LAWP.2018.2890790
15. Kumar A, Chaturvedi D, Raghavan S. Design and experimental verification of dual-fed, self-diplexed cavity-backed slot antenna using HMSIW technique. *IET Microw Antennas Propag*. 2019;13:380-385. doi:10.1049/iet-map.2018.5327
16. Kumar A, Raghavan S. Planar cavity-backed self-diplexing antenna using two-layered structure. *Prog Electromagn Res Lett*. 2018;76:91-96. doi:10.2528/PIERL18031605
17. Nandi S, Mohan A. SIW-based cavity-backed self-diplexing antenna with plus-shaped slot. *Microw Opt Technol Lett*. 2018;60(4):827-834. doi:10.1002/mop.31067
18. Wu Q, Yin J, Yu C, Wang H, Hong W. Low-profile millimeter-wave SIW cavity-backed dual-band circularly polarized antenna. *IEEE Trans Antennas Propag*. 2017;65(12):7310-7315. doi:10.1109/TAP.2017.2758165
19. Wu Q, Wang H, Yu C, Hong W. Low-profile circularly polarized cavity-backed antennas using SIW techniques. *IEEE Trans Antennas Propag*. 2016;64(7):2832-2839. doi:10.1109/TAP.2016.2560940
20. Vasina P, Lacik J. Circularly polarized rectangular ring-slot antenna with chamfered corners for off-body communication at 5.8 GHz ISM band. *Radioengineering*. 2017;26(1):85-90. doi:10.13164/re.2017.0085
21. Liang T, Wang Z, Dong Y. A circularly polarized SIW slot antenna based on high-order dual-mode cavity. *IEEE Antennas Wirel Propag Lett*. 2020;19(3):388-392. doi:10.1109/LAWP.2020.2972115
22. Xu Y, Wang Z, Dong Y. Circularly polarized slot antennas with dual-mode elliptic cavity. *IEEE Antennas Wirel Propag Lett*. 2020;19(4):715-719. doi:10.1109/LAWP.2020.2978343
23. Li W, Tang XH, Yang Y. A K_a-band circularly polarized substrate integrated cavity-backed antenna Array. *IEEE Antennas Wirel Propag Lett*. 2019;18(9):1882-1886. doi:10.1109/LAWP.2019.2932111
24. Huang J, Qiu F, Lin W, et al. A new compact and high gain circularly-polarized slot antenna Array for K_u-band Mobile satellite TV reception. *IEEE Access*. 2017;5:6707-6714. doi:10.1109/ACCESS.2017.2694229
25. Priya S, Kumar K, Dwari S, Mandal MK. Circularly polarized self-diplexing SIW cavity backed slot antennas. *IEEE Trans Antennas Propag*. 2020;68(3):2387-2392. doi:10.1109/TAP.2019.2938576
26. Deslandes D, Wu K. Design consideration and performance analysis of substrate integrated waveguide components. 2002 32nd European Microwave Conference; 2002, pp. 1–4. doi:10.1109/EUMA.2002.339426
27. Entesari K, Saghati AP, Sekar V, Armendariz M. Tunable SIW structures: antennas, VCOs, and filters. *IEEE Microw Mag*. 2015;16(5):34-54. doi:10.1109/MMM.2015.2408273
28. Kumar M, Nath V. Microstrip-line-fed elliptical wide-slot antenna with similar parasitic patch for multiband applications. *IET Microw, Antennas Propag*. 2018;12:2172-2178. doi:10.1049/iet-map.2018.5377
29. Kretzschmar JG. Wave propagation in hollow conducting elliptical waveguides. *IEEE Trans Microw Theory Tech*. 1970;18(9):547-554. doi:10.1109/TMTT.1970.1127288
30. Zheng Q, Guo C, Li H, Ding J. Wideband and high efficiency reflective polarization rotator based on metasurface. *J Electromagn Waves Appl*. 2018;32(3):265-273. doi:10.1080/09205071.2017.1377640
31. Iqbal A, Saraereh A, Bouazizi A, Basir A. Metamaterial-based highly isolated MIMO antenna for portable wireless applications. *Electronics*. 2018;7(10):267. doi:10.3390/electronics7100267

AUTHOR BIOGRAPHIES

Amit Kumar was born in Agra, Uttar Pradesh, India, in 1993. He received his B.Tech degree in Electronics and Communication Engineering from Ambedkar Institute of Advanced Communication Technologies and Research, affiliated to Guru Gobind Singh Indraprastha University (GGSIPU), India, in 2014 and masters in Electronics and Communication (ECE) from University School of Information, Communication and Technology (USIC&T), Guru Gobind Singh Indraprastha University (GGSIPU), India, in 2016. He is currently pursuing his Ph.D. from IIT (BHU), Varanasi, India. His research interests include SIW-based antennas and circuits, broadband antennas, circularly polarized antennas MMW, and THz Bands.

Munish Kumar was born in New Delhi, India, in 1990. He received his M.Tech in ECE from USIC&T, GGSIPU, India, in 2015. He is currently pursuing his Ph.D. from USIC&T, GGSIPU, New Delhi, India. He has worked extensively and authored more than 20 research articles on multiband and wideband microstrip patch antennas, fractals, electromagnetic bandgap structures (EBG), circularly polarized and MIMO antennas in various international journals and conferences. His current research involves designing of microstrip antennas for wideband and multiband applications.

Amit Kumar Singh received the Ph.D. degree from the IIT (BHU) Varanasi in 2010, respectively. He was working as Associate Professor in the Electronics Engineering department in IIT (BHU) since 2012. His research interest includes the areas of design of millimeter frequency antennas, feeds for parabolic reflectors, dielectric resonator

antennas, microstrip antennas, EBG, artificial magnetic conductors, soft and hard surfaces, Antennas for RFIDs, phased array antennas, and computer aided design for antennas. He has published and co-authored over 70 journal articles and conference articles.

How to cite this article: Kumar A, Kumar M, Singh AK. A dual-band dual-sense circularly polarized self-diplexing SIW cavity-backed antenna with elliptical slot for millimeter-wave 5G applications. *Int J RF Microw Comput Aided Eng*. 2022;32(10):e23297. doi:10.1002/mmce.23297